3-1-2023

Differences in Startle and Prepulse Inhibition in Contactin-associated Protein-like 2 Knock-out Rats are Associated with Sex-specific Alterations in Brainstem Neural Activity

Alice Zheng

Kaela E Scott

Ashley L Schormans

Rajkamalpreet Mann

Brian L Allman

See next page for additional authors

NEUROSCIENCE
RESEARCH ARTICLE
A. Zheng et al. / Neuroscience 513 (2023) 96–110

Differences in Startle and Prepulse Inhibition in Contactin-associated Protein-like 2 Knock-out Rats are Associated with Sex-specific Alterations in Brainstem Neural Activity

Alice Zheng, Kaela E. Scott, Ashley L. Schormans, Rajkamalpreet Mann, Brian L. Allman [†] and Susanne Schmid [*†]

Anatomy & Cell Biology, Schulich School of Medicine & Dentistry, University of Western Ontario, Canada

Abstract—The contactin-associated protein-like 2 (*CNTNAP2*) gene encodes for the CASPR2 protein, which plays an essential role in neurodevelopment. Mutations in *CNTNAP2* are associated with neurodevelopmental disorders, including autism spectrum disorder and schizophrenia. Rats with a loss of function mutation in the *Cntnap2* gene show increased acoustic startle response (ASR) and decreased prepulse inhibition (PPI). The neural basis of this altered auditory processing in *Cntnap2* knock-out rats is currently unknown. Auditory brainstem recordings previously revealed no differences between the genotypes. The next step is to investigate brainstem structures outside of the primary auditory pathway that mediate ASR and PPI, which are the pontine reticular nucleus (PnC) and pedunculopontine tegmentum (PPTg), respectively. Multi-unit responses from the PnC and PPTg *in vivo* of the same rats revealed sex-specific effects of loss of CASPR2 expression on PnC activity, but no effects on PPTg activity. Female *Cntnap2*$^{-/-}$ rats showed considerably increased PnC firing rates compared with female wildtypes, whereas the difference between the genotypes was modest in male rats. In contrast, for both females and males we found meager differences between the genotypes for PPTg firing rates and inhibition of PnC firing rates, indicating that altered firing rates of these brainstem structures are not responsible for decreased PPI in *Cntnap2*$^{-/-}$ rats. We conclude that the auditory processing changes seen in *Cntnap2*$^{-/-}$ rats are associated with, but cannot be fully explained by, differences in PnC firing rates, and that a loss of function mutation in the *Cntnap2* gene has differential effects depending on sex.

Key words: sensorimotor gating, autism, neurodevelopmental disorder, electrophysiology, neural mechanism.

INTRODUCTION

The contactin-associated protein-like 2 gene, *CNTNAP2*, is an essential gene for neuronal development (Anderson et al., 2012) that is highly expressed in sensory brain regions (Gordon et al., 2016). Mutations in *CNTNAP2* are associated with many neurodevelopmental disorders such as autism spectrum disorder, schizophrenia, and intellectual disability (Rodenas-Cuadrado et al., 2014). CASPR2, the protein product of *CNTNAP2*, is a neurexin-like protein involved in the clustering of voltage-gated potassium channels in the juxtaparanodal region of myelinated axons (Poliak et al., 1999). CASPR2 is important during development, playing a role in neuronal migration (Strauss et al., 2006); in dendritic arborization, spine development, and synaptic stabilization (Anderson et al., 2012); and in determining firing rates and network activities (Peñagarikano et al., 2011). Previous studies from our lab showed that rats with a loss of function mutation in the *Cntnap2* gene have increased reactivity to sound as measured through the acoustic startle response (ASR) and decreased sensorimotor gating as measured through prepulse inhibition (PPI; Möhrle et al., 2021; Scott et al., 2018, 2020), paralleling similar findings in autistic people and people with schizophrenia (Erturk et al., 2016; Cheng et al., 2018; Swerdlow et al., 2018). Given the face and construct validity of the *Cntnap2*$^{-/-}$ rat model, this provides an opportunity to further investigate the neural mechanisms underlying disruptions in ASR and PPI, and therefore to better understand the neural basis of altered sensory processing in neurodevelopmental disorders.

In considering how a functional loss of *Cntnap2* could contribute to disruptions in ASR and PPI, it is important to note that CASPR2 is normally expressed in the cochlear

*Corresponding author. Address: Anatomy & Cell Biology, Schulich School of Medicine & Dentistry, University of Western Ontario, London, ON N6A 5C1, Canada.
E-mail address: susanne.schmid@schulich.uwo.ca (S. Schmid).
† Co-Senior authors.

Abbreviations: CNTNAP2, contactin-associated protein-like 2; ASR, acoustic startle response; PPI, prepulse inhibition; PnC, pontine reticular nucleus; PPTg, pedunculopontine tegmentum; ABR, auditory brainstem response; CRNs, cochlear root neurons; MN, motor neurons; CN, cochlear nucleus; IC, inferior colliculus; SC, superior colliculus; SPL, sound pressure level; ISI, inter-stimulus interval; PSTH, peristimulus time histogram; SD, standard deviation; PFA, paraformaldehyde; PBS, phosphate-buffered saline.

https://doi.org/10.1016/j.neuroscience.2023.01.020
0306-4522/

nucleus, inferior colliculus, and superior olivary complex (Gordon et al., 2016), as well as the pontine reticular nucleus (PnC) and the pedunculopontine tegmental nucleus (PPTg; Scott et al., 2018), brain regions known to participate in ASR and/or PPI. The primary ASR neural pathway involves cochlear root neurons, giant neurons in the PnC, and motor neurons (Lee et al., 1996; Lingenhöhl and Friauf, 1994; Fig. 1). After receiving signals from spiral ganglion cells in the inner ear, cochlear root neurons innervate PnC giant neurons, which then activate motor neurons, ultimately causing the muscle contractions of the startle response (Lingenhöhl and Friauf, 1994). The proposed PPI neural pathway involves cochlear neurons projecting to the inferior colliculus, which then signals to the superior colliculus, which signals to the PPTg (Koch, 1999). The PPTg is thought to then mediate PPI through sending inhibitory signals to the PnC (Koch, 1999).

In our first effort to understand the disruptions in ASR and PPI observed in *Cntnap2*$^{-/-}$ rats, we previously recorded the auditory brainstem response (ABR) in homozygously-bred *Cntnap2*$^{-/-}$ rats (Scott et al., 2018) to investigate if the disruptions were due to alterations in the magnitude or speed at which sound-evoked activity is relayed through the auditory pathway (i.e., from the auditory nerve to the inferior colliculus). Although adult *Cntnap2*$^{-/-}$ rats showed exaggerated ASRs and reduced PPI compared with wildtypes, they did not demonstrate differences in their hearing thresholds to acoustic stimuli, nor did they show increased sound-evoked activity along their successive auditory nuclei that could directly explain their ASR and PPI results (Scott et al., 2018). Furthermore, recent work in our lab has found no differences between the genotypes for amplitudes or latencies of the ABR in juvenile, adolescent, and adult wildtype and *Cntnap2*$^{-/-}$ rats when bred heterozygously and compared between littermates (unpublished data). Taken together, these ABR data on homozygously- and heterozygously-bred *Cntnap2*$^{-/-}$ rats suggest that *Cntnap2*-related disruptions in acoustic reactivity (e.g., ASR) and sensorimotor gating (e.g., PPI) are unlikely to be due to differences in auditory processing at the level of the cochlea, auditory nerve, or cochlear nucleus. Instead, downstream structures in the ASR/PPI pathways, such as the PnC or PPTg, could be affected in *Cntnap2*$^{-/-}$ rats. This working hypothesis is further supported by the finding of alterations in the relative levels of glutamine, glutamate, and GABA in the PnC of *Cntnap2*$^{-/-}$ rats compared with wildtype rats (Möhrle et al., 2021). Thus, the PnC and PPTg are promising candidate brain regions within the ASR/PPI pathways that may be involved in altered sensorimotor processing in *Cntnap2*$^{-/-}$ rats.

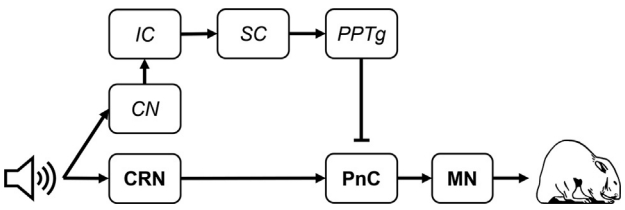

Fig. 1. Brain regions involved in the acoustic startle response (ASR) pathway and prepulse inhibition (PPI) pathway. **Bold**: Primary ASR pathway. Cochlear root neurons (CRNs) project to giant neurons in the caudal pontine reticular nucleus (PnC), which project to spinal cord motor neurons (MN) that elicit the startle response. *Italics*: Proposed major PPI pathway. Neurons in the cochlear nucleus (CN) project to the inferior colliculus (IC), which projects to the superior colliculus (SC). The SC then signals to the pedunculopontine tegmental nucleus (PPTg), and PPTg neurons send inhibitory signals to PnC giant neurons. Modified from Azzopardi et al. (2018).

In the present study, we used a combination of behavioural startle experiments and *in vivo* extracellular electrophysiological recordings to investigate sound-evoked activity in the PnC and PPTg in adult, heterozygously-bred *Cntnap2*$^{-/-}$ rats and littermate wildtype controls. We hypothesized that the increased ASR and decreased PPI observed in *Cntnap2*$^{-/-}$ rats are due to increased sound-evoked PnC activity and decreased inhibition by prepulse-evoked PPTg activity, respectively.

EXPERIMENTAL PROCEDURES

Animals

Both female and male rats were used for all experiments, aged post-natal day 68 (p68) to p83 for behavioural experiments and p72 to p94 for electrophysiological recordings. Sprague-Dawley wildtype (*Cntnap2*$^{+/+}$) and homozygous *Cntnap2* knock-out (*Cntnap2*$^{-/-}$) rats from 12 different litters (1-3 pups from each litter) were obtained from heterozygous (*Cntnap*$^{+/-}$) crossings. *Cntnap*$^{+/-}$ breeders were obtained from Horizon Discovery (Boyertown, PA, USA). Date of birth was designated as post-natal day zero (p0). Rats were weaned on p21, and sexes were separated on p35. Rats were housed in a temperature-controlled room on a 12-h light/dark cycle (lights on at 07:00 h), with *ad libitum* food and water. Behavioural testing was performed during the light phase. All procedures were approved by the University of Western Ontario Animal Care Committee and were in accordance with the guidelines established by the Canadian Council on Animal Care.

Acoustic reactivity and sensorimotor gating - behavioural testing

Startle magnitude was measured using sound-attenuating startle boxes (LE116; Panlab) using the StartFear system (Panlab) and STARTLE software module (PACKWIN-CSST, PACKWIN version 2.0; Panlab). Rats were placed in a movement-limiting tube on a motion-sensitive platform in the sound-attenuating chamber. Rats were acclimated to the testing room and testing boxes prior to all testing paradigms. For all paradigms, trials were separated by 12, 15, or 18 second inter-trial intervals. The order of presentation of acoustic stimuli was randomized for all testing paradigms, as was the order of testing for wildtype rats versus *Cntnap2*$^{-/-}$ rats. Different testing paradigms were separated by 1 hour or more to allow for recovery from the previous testing paradigm. All startle pulses and prepulses had a 5-ms rise/fall time.

Rats were first acclimated to a background sound of 60 dB sound pressure level (SPL). ASR was tested with 20-ms 62–110 dB SPL startle pulses in 6 dB steps, which were presented 10 times per sound level in a randomized order. Startle threshold (25% of maximum startle) of each rat was calculated by scaling the function of the startle response to the different sound levels, then fitting the scaled function and solving for threshold as described in Möhrle et al. (2021). The next day, sensorimotor gating was assessed using a PPI paradigm. PPI was tested with 20-ms 105 dB SPL startle pulses preceded by 10-ms 65 to 89 dB SPL prepulses, in 6 dB steps. Prepulses and startle pulses were separated by 100-ms inter-stimulus intervals (ISIs). Each prepulse sound level was presented 20 times in a randomized order, including trials of 105 dB SPL startle pulse with no prepulse (0 dB prepulse). Percent prepulse inhibition (%PPI) was calculated with the following equation:

$$\%\ PPI = \left(1 - \frac{startle\ magnitude\ (arb.)\ prepulse\ condition}{startle\ magnitude\ (arb.)\ no\ prepulse\ condition}\right) \times 100\%$$

Startle magnitude in response to different intensities of startle pulses was calculated for each rat by averaging the startle magnitude across the 10 trials for each startle pulse sound level. Percent PPI for varying prepulse intensities was likewise calculated by averaging %PPI across the 20 trials for each prepulse sound level.

Electrophysiological recordings

Immediately following ABR recordings (Supplementary Materials), rats were maintained under ketamine (80 mg/kg IP) and xylazine (5 mg/kg IP) so that they could be prepped for *in vivo* extracellular electrophysiology recordings. The custom foam earplug was removed from the left ear and rats were positioned in a stereotaxic frame with a nose clamp and blunt ear bars.

Surgical procedure. A midline incision was made in the skin, and the underlying tissue was reflected from the skull so that two craniotomies could be performed. The first was in the caudal aspect of the left parietal bone in order to expose the cortical tissue dorsal to the PPTg (2.0 mm × 3.0 mm; 6.5–8.5 caudal to bregma and 1.0–4.0 lateral to the midline). The second was in the left side of the occipital bone to expose the cortical tissue dorsal to the PnC (2.5 mm × 3.0 mm; 10.5–13.0 caudal to bregma and 0.0–3.0 lateral to the midline). A stainless-steel screw was inserted into the right frontal bone, to which a ground wire was connected. Having used dental acrylic to secure a headpost to the skull, at the end of the surgical procedure both ear bars were removed to allow for biaural free-field auditory stimulation during the simultaneous electrophysiological recordings in the PnC and PPTg. The rat remained in the stereotaxic frame using the headpost and nose clamp for the remainder of the experiment.

Recording equipment. Using a high-precision stereotaxic manipulator (World Precision Instruments, Sarasota, FL), 32-channel electrode arrays were separately inserted into the PnC and PPTg. To best sample neurons from the respective brain regions, a laminar electrode array (A1x32-5 mm-25–177; NeuroNexus Technologies, Ann Arbor, MI) was used for PnC recordings, whereas a Poly2 electrode array (A1x32-Poly2-5 mm-50 s-177; NeuroNexus Technologies, Ann Arbor, MI) was used for PPTg recordings. Each electrode array consisted of 32 channels which recorded multi-unit activity via a high impedance headstage (NN32AC; TDT). The neuronal activity was preamplified and digitized (two RA16SD Medusa preamps; TDT) and sent to a RZ5 processing module via a fiber optic cable. Multi-unit activity was digitally sampled at 25 kHz and bandpass filtered online at 300–3000 Hz for spiking data. A voltage threshold of three standard deviations above the noise floor was used for spike detection.

Recording sites. For PnC recordings, electrode penetrations were targeted between 9.4 and 10.0 mm caudal to bregma. This was achieved by positioning the electrode array entry at 11.6 to 12.2 mm caudal to bregma, 1.2 mm lateral to the midline, and 8400–8600 μm depth, with an entry angle of 16° caudal from the vertical plane. For PPTg recordings, electrode penetrations were targeted between 7.6 and 8.3 mm caudal to bregma, with a vertical entry angle positioned 2.0 mm lateral to the midline and 6700–6800 μm depth. Once the electrode arrays were in position, the brain was allowed to recover for 40 minutes to 1 hour before acoustic stimulation paradigms began. Electrodes were dipped in Vibrant DiI Red (V22885; Molecular Probes, Inc., Eugene, OR) before introduction into the brain, for marking the recording sites.

Acoustic stimulation paradigms. Acoustic stimulation paradigms were performed simultaneously for the PnC and PPTg. Auditory stimulation paradigms were presented using a RZ6 processing module (TDT; 100 kHz sampling rate) and custom MATLAB scripts (R2020a; The MathWorks). Speakers were positioned 20 cm above and 24 cm in front of the rat's head, in line with the body midline such that the total distance from the rat's ears was 28.3 cm at an angle of 32° above the horizontal plane. For all paradigms, background noise of 60 dB SPL was delivered using a magnetic speaker (MF1; TDT). Acoustic stimulation paradigms were consistent with the above-mentioned behavioural experiments. In brief, the electrophysiological response to an ASR paradigm was tested with 20-ms, 62–110 dB SPL startle pulses presented 10 times per sound level in a randomized order. Startle stimuli (1–32 kHz noise bursts) for the ASR paradigm were delivered using a super tweeter (T90A; Fostex). The electrophysiological response to a PPI paradigm was tested with 20-ms, 105 dB SPL startle pulses preceded by 10-ms, 65 to 89 dB SPL prepulses presented 20 times per prepulse sound level in a randomized order, with 100-ms ISIs.

Prepulse stimuli (1–32 kHz noise bursts) for the PPI paradigm were delivered using a magnetic speaker (MF1; TDT). Startle stimuli (1–32 kHz noise bursts) for the PPI paradigm were delivered using a super tweeter (T90A; Fostex).

Confirmation of electrode hits. Once the electrophysiological recordings were finished, the electrode arrays were withdrawn, and the rat was removed from the stereotaxic frame. The rat was then prepped for exsanguination and transcardial perfusion, and the brain was harvested for slicing and histological analysis (Supplementary Materials). For each electrode penetration, the electrode array location was matched with the corresponding anatomical location using *The Rat Brain in Stereotaxic Coordinates* (Paxinos and Watson, 2007) to create a histological reconstruction (Fig. 2A, B). For the PnC, the electrodes were positioned between 9.36 and 10.08 mm caudal to bregma. PnC penetrations that hit within an area that contained giant neurons (> 30 μm soma diameter) were included in analysis (Fig. 2C). For the PPTg, the electrodes were positioned between 7.56 and 8.28 mm caudal to bregma. PPTg penetrations that hit within an area with cholinergic cells were included in analysis (Fig. 2D).

Offline analysis of multi-unit activity

Using custom MATLAB scripts (R2020b, MathWorks), rasters and peristimulus time histograms (PSTHs) were generated for each channel (Fig. 3, Supplementary Fig. 3D). PSTHs were created by grouping spikes into 2-ms bins. For all testing paradigms, spontaneous activity for each channel was found by calculating the firing rate in the last 500 ms of each trial, then averaging the firing rates across all trials. Firing rates for each channel in response to the acoustic stimuli was calculated as the number of spikes between 2-ms and 40-ms after stimulus onset, divided by 38-ms, averaged across all trials for each sound level. For the PPI paradigm, the percent reduction in PnC firing rate was calculated as:

$$\%\ reduction\ in\ firing\ rate = \left(1 - \frac{firing\ rate\ (Hz)\ prepulse\ condition}{firing\ rate\ (Hz)\ no\ prepulse\ condition}\right) \times 100\%$$

Responsivity for each channel was found using a t-test on MATLAB (R2020b, MathWorks) to determine if the firing rates at each startle pulse sound level were significantly above spontaneous activity for that channel. For the ASR paradigm, threshold for each channel was determined as the lowest startle pulse sound level at

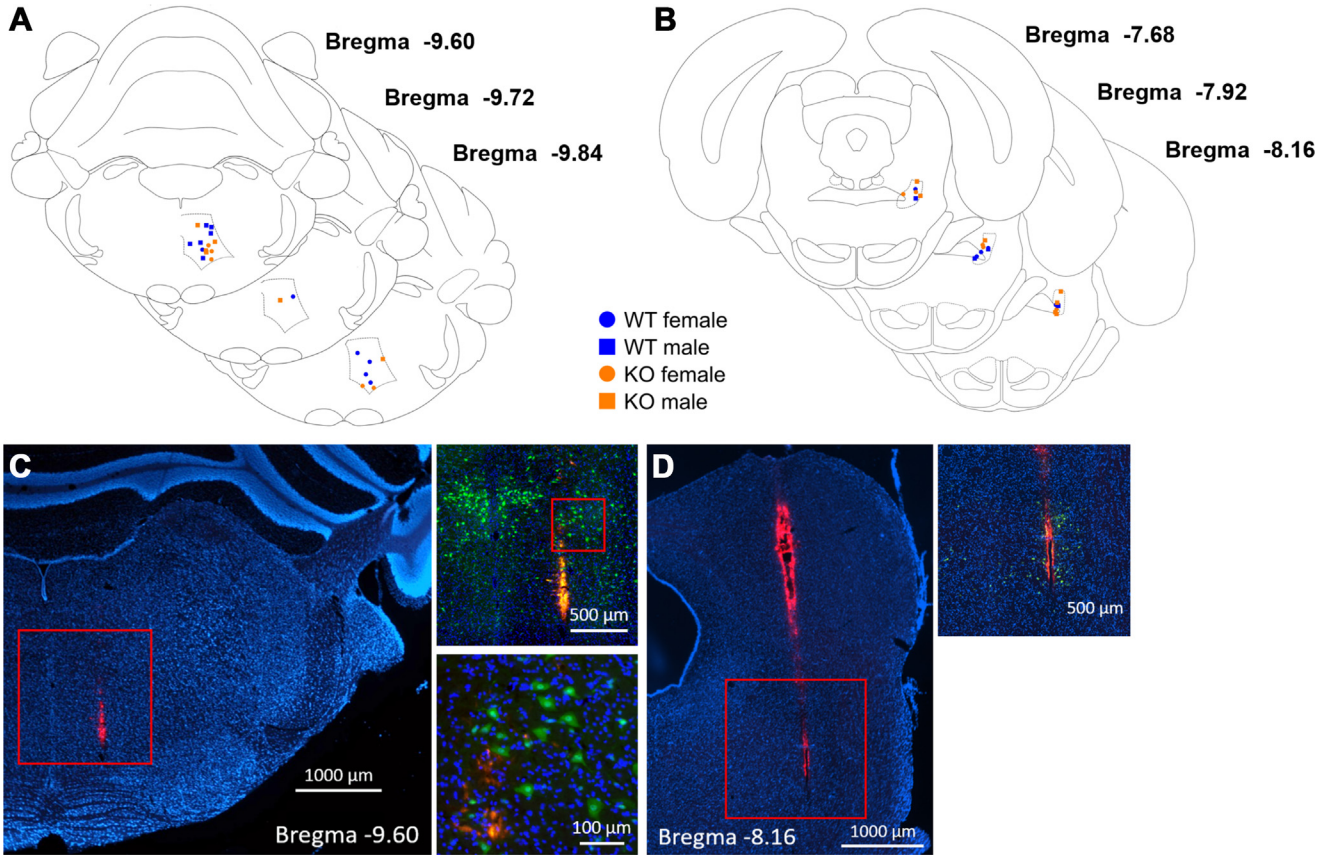

Fig. 2. A reconstruction of successful electrode hits for *in vivo* extracellular electrophysiological recordings in the PnC (**A**; wildtype, $N = 12$; *Cntnap2*$^{-/-}$, $N = 11$) and PPTg (**B**; wildtype, $N = 10$; *Cntnap2*$^{-/-}$, $N = 12$). Dots indicate the most distal DiI trace of each electrode. Modified from Paxinos and Watson (2007). **(C)** Representative image of a PnC hit. Blue = DAPI. Red = DiI. Green = NeuN. **(D)** Representative image of a PPTg hit. Blue = DAPI. Red = DiI. Green = NOS1.

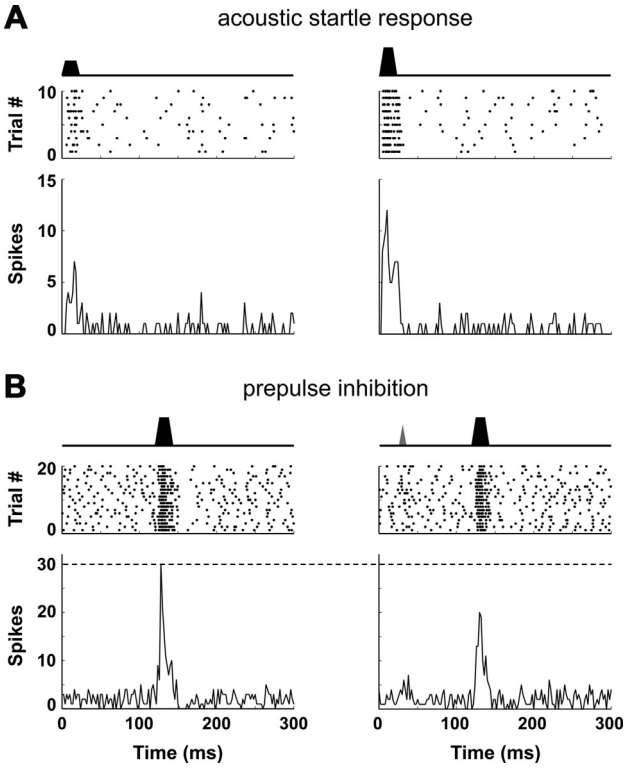

Fig. 3. Methodological comparison of the ASR paradigm and the PPI paradigm performed during the electrophysiological recordings. Each panel shows a representative dot raster plot and peristimulus time histogram (PSTH) from a male wildtype rat in response to the given paradigm. For the dot raster plots, each dot represents a spike. For the PSTHs, spikes were grouped into 2-ms bins. **(A)** PnC response from a single channel in response to 80 dB SPL sound pulse (left) and 110 dB SPL startle pulse (right), showing that the magnitude of the PnC response increased at the higher sound intensity. **(B)** PnC response from a single channel in response to a 105 dB SPL startle pulse preceded by no prepulse (left) and preceded by 77 dB SPL prepulse (right). The dashed line at 30 spikes shows the decrease in number of spikes for the prepulse condition (right) compared with the no prepulse condition (left).

which the channel was consistently responsive. If a channel was not responsive to any of the sound intensities, that channel was considered non-responsive and was removed from analysis. Response onsets, offsets, and durations were calculated for the sound levels at which a channel was deemed responsive. Response onset was determined as when the firing rate was consistently two standard deviations or more above the spontaneous firing rate. Response offset was determined as when firing rate returned to spontaneous activity. Response duration was calculated as response onset subtracted from response offset. To calculate the firing rates per rat, firing rates in the PnC and PPTg for each sound level were averaged across the 32 respective channels on the electrode array, excluding channels that were non-responsive to sound from the ASR testing block. Firing rate thresholds per rat were then calculated by averaging the PnC thresholds across the 32 respective channels, excluding channels that were non-responsive. The % reduction in PnC firing rate for each prepulse level was calculated for each rat by averaging the % reduction in PnC firing rate from each of the 32 respective channels, excluding channels that were non-responsive to sound from the ASR testing block and a few channels that were non-responsive to the no prepulse condition from the PPI testing block.

Statistical analysis

A 3-way mixed ANOVA was separately performed for the following metrics: ABR amplitudes, ABR latencies, startle magnitudes, firing rates, normalized firing rates, %PPI, and % reduction in firing rates across sound levels. Greenhouse-Geisser correction was used when sphericity was violated. When there was no significant 3-way interaction, 2-way interactions involving genotype are reported. Main effects are reported when no interactions involving genotype were found. If there was a significant 3-way interaction, *post hoc* 2-way ANOVAs were performed separately for females and males. If there was a significant 2-way interaction involving genotype, t-test with Bonferroni correction was performed to investigate differences between the genotypes at specific sound levels. A mixed-effects analysis was separately performed for response onset latencies and response durations. For threshold values, 2-way ANOVAs were performed. For assessment of the correlation between startle magnitudes and PnC firing rates, Pearson's correlation was performed. Graphs show mean ± standard deviation (SD). Statistically significant differences were considered at p-values less than $\alpha = 0.05$. Statistical analyses were either run on IBM SPSS Statistics 26 (IBM Corp., Armonk, N.Y., USA) or GraphPad Prism 8.3.0 (GraphPad Software, San Diego, CA). All graphs were generated on GraphPad Prism 8.3.0 (GraphPad Software, San Diego, CA). All figures were completed with Inkscape (Inkscape 0.92.5).

RESULTS

ABR recordings

To confirm that the *Cntnap2*-related alterations in acoustic reactivity and sensorimotor gating do not arise from differences in the sound-evoked activity in the brainstem auditory pathway (Scott et al., 2018), we recorded ABR signals in response to 0.1-ms clicks decreasing from 89 to 41 dB SPL, in 6 dB steps. Peak I amplitude, which corresponds to synchronized activity at the level of the auditory nerve, was determined in reference to a baseline of 0 μV. Latency to peak I was determined as time to peak I amplitude from stimulus onset. There were no significant interactions involving genotype for peak I amplitudes as well as no significant main effect of genotype for peak I amplitudes (main effect of genotype: $F(1, 22) = 0.3160$, $P = 0.5797$; Supplementary Fig. 1B). A significant 3-way interaction (sex × genotype × sound level) was observed ($F(8, 176) = 3.689$, $P = 0.0005$) for peak I latencies. For females, there was a significant 2-way interaction between genotype and sound level ($F(8, 88) = 2.784$, $P = 0.0086$), but post-hoc comparisons did not reveal

any significant differences between the genotypes at specific sound levels (Supplementary Fig. 1C). For males, there was also a significant 2-way interaction between genotype and sound level ($F(8, 88) = 3.043$, $P = 0.0045$), but again post-hoc comparisons did not reveal any significant differences between the genotypes at specific sound levels (Supplementary Fig. 1C). Taken together, these ABR peak I amplitude and latency data suggest that any alterations in the ASR and PPI in *Cntnap2*$^{-/-}$ rats are likely not due to deficits in the processing of sensory input into the startle pathway. Additionally, amplitudes and latencies of later peaks of the ABR (corresponding to activity in the cochlear nucleus - peak II; superior olivary complex - peak III; and lateral lemniscus pathway to the inferior colliculus - peak IV) did not differ between genotypes (data not shown).

Startle responses and neural activity in the PnC

Acoustic startle responses were tested by presenting 10 trials of 20-ms startle pulses ranging from 62 to 110 dB SPL, in 6 dB steps, in a randomized order. Respective multiunit firing rates in response to 20-ms startle pulses were calculated by dividing the total number of spikes 2-ms to 40-ms after stimulus onset by 38 ms. The minimum number of multiunit channels that were responsive to sound for an individual rat was 25 in the PnC and 27 in the PPTg. The maximum number of multiunit channels that were responsive to sound for an individual rat was 32 in the PnC and 32 in the PPTg.

For startle magnitudes, there was a significant genotype × sound level interaction ($F(8, 176) = 5.900$, $P < 0.0001$). Post-hoc tests revealed significantly increased startle magnitudes of *Cntnap2*$^{-/-}$ rats compared with wildtype rats at 86 dB SPL ($P = 0.0127$) and 92 dB SPL ($P = 0.0010$; Fig. 4A). In

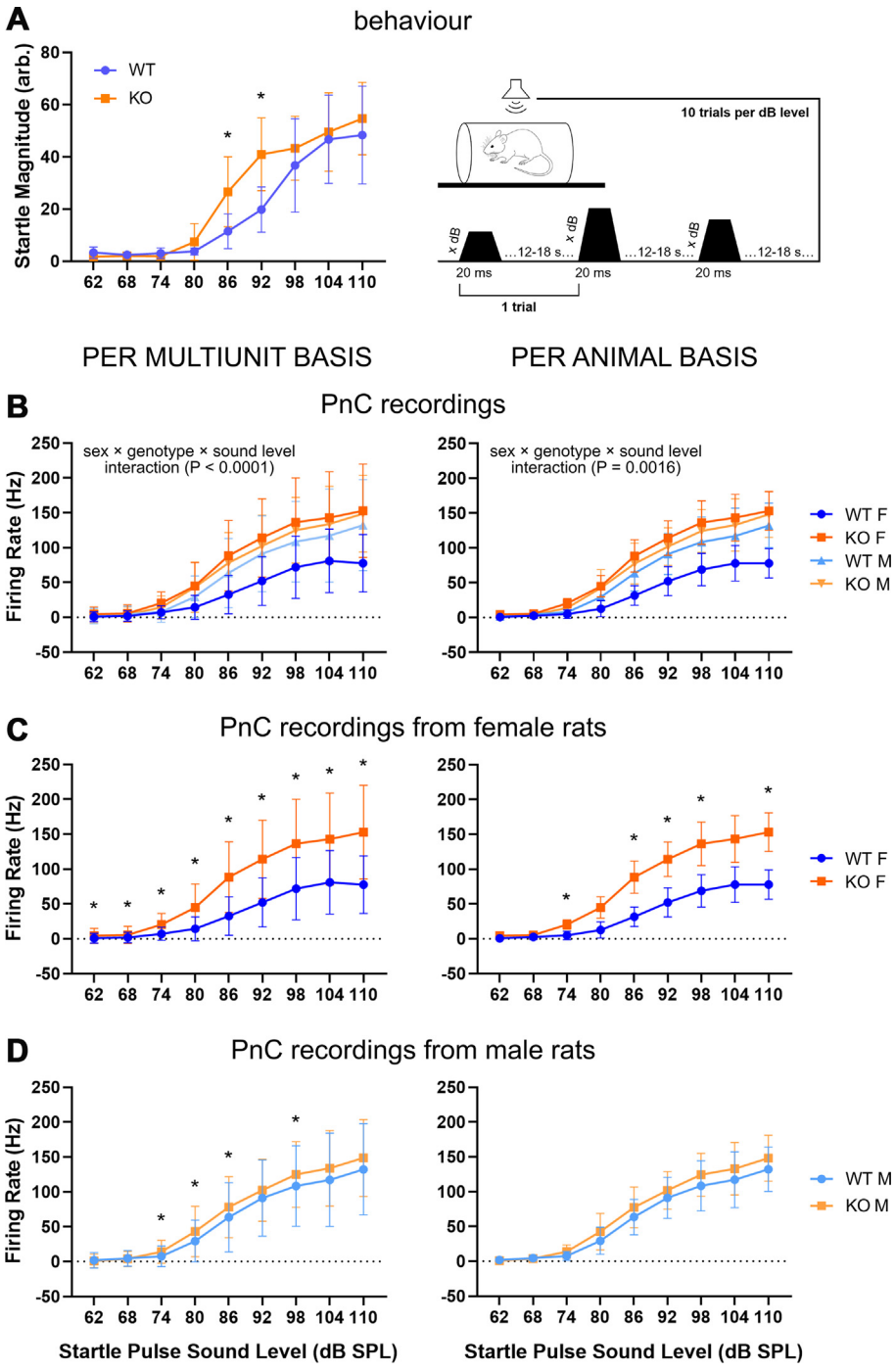

Fig. 4. Increased reactivity to acoustic stimuli was accompanied by increased firing rates in the PnC of *Cntnap2*$^{-/-}$ rats compared with wildtype rats. **(A)** Acoustic startle stimuli ranging from 62 to 110 dB SPL, in 6 dB steps, were presented 10 times per sound level with 12–18 second inter-trial intervals. At 86 and 92 dB SPL, startle magnitudes were significantly higher in *Cntnap2*$^{-/-}$ rats ($P < 0.05$) compared with wildtypes. **(B)** For both the multiunit and animal basis, there was a significant 3-way interaction of sex × genotype × sound level. **(C)** Firing rates in the PnC were significantly higher in *Cntnap2*$^{-/-}$ females ($P < 0.05$) compared with wildtype females, when analyzed on both a multiunit basis and an animal basis. **(D)** When analyzed on a per multiunit basis, firing rates in the PnC were higher in *Cntnap2*$^{-/-}$ males ($P < 0.05$) compared with wildtype males. However, when analyzed on a per animal basis, there were no significant differences between the genotypes in male rats. Wildtype: $N = 12$ rats; PnC = 177 multiunits from 6 females, 192 multiunits from 6 males. *Cntnap2*$^{-/-}$: $N = 14$ rats; PnC = 157 multiunits from 5 females, 188 multiunits from 6 males. Graphs show mean ± SD. *$P < 0.05$.

respective PnC recordings, a significant 3-way interaction was found for the multiunit data (sex × genotype × sound level interaction: F(8, 5248) = 25.97, $P < 0.0001$; Fig. 4B). For females, there was a significant 2-way interaction between genotype and sound level (F(8, 2224) = 78.26, $P < 0.0001$) and post-hoc tests revealed significantly increased firing rates in *Cntnap2*$^{-/-}$ females compared with wildtype females at all sound levels tested ($P < 0.05$; Fig. 4C). For males, there was also a significant 2-way interaction between genotype and sound level (F(8, 3024) = 6.012, $P < 0.0001$) and post-hoc tests revealed significantly increased firing rates in *Cntnap2*$^{-/-}$ males compared with wildtype males at 74, 80, 86, and 98 dB SPL ($P < 0.05$; Fig. 4D).

The difference between the genotypes for multiunit data from males was modest, so further analyses were run to compare the averages per animal against the raw multiunit data. Indeed, the modest difference between wildtype and *Cntnap2*$^{-/-}$ males observed in the multiunit analysis became insignificant when run on a per animal basis. Per animal, there was again a significant 3-way interaction (sex × genotype × sound level interaction: F(8, 152) = 3.326, $P = 0.0016$; Fig. 4B). For female rats, there was a significant 2-way interaction between genotype and sound level (F(8, 72) = 12.40, $P < 0.0001$). Post-hoc tests revealed significantly increased firing rates in female *Cntnap2*$^{-/-}$ rats compared with female wildtype rats at 74, 86, 92, 98, and 110 dB SPL ($P < 0.05$; Fig. 4C). Additionally, increased PnC firing rates in female *Cntnap2*$^{-/-}$ rats appear to be disproportionately elevated relative to their increased startle magnitudes, such that female wildtype rats have higher startle than female *Cntnap2*$^{-/-}$ rats at the same PnC firing rate (Supplementary Fig. 2A). This correlation could not be run on a multiunit basis because there is no multiunit equivalent for behavioural startle magnitudes. Finally, in contrast to the multiunit analysis, males did not show a significant 2-way interaction or significant differences between the genotypes for PnC firing rates (main effect of genotype: F(1, 10) = 0.710, $P = 0.419$; Fig. 4D).

To further investigate the PnC firing rate differences between wildtype and *Cntnap2*$^{-/-}$ rats in females and males, PnC firing rates were normalized to the firing rate at 110 dB. Normalizing the firing rates allows us to distinguish between a simple increase of PnC firing rates (i.e., startle-scaling) and a leftward shift of the input/output function (i.e., sound-scaling), which represent different components of sensory processing (Miller et al., 2021). For the multiunit analysis, there was a significant 2-way interaction between genotype and sound level for both females (F(8, 2536) = 14.64, $P < 0.0001$) and males (F(8, 3000) = 5.003, $P < 0.0001$). *Cntnap2*$^{-/-}$ females had significantly increased normalized firing rates compared with wildtype females at 74, 80, 86, and 92 dB SPL ($P < 0.05$; Fig. 5A). *Cntnap2*$^{-/-}$ males had significantly increased normalized firing rates compared with wildtype males at 80 and 86 dB SPL ($P < 0.05$; Fig. 5B). When analyzed on a per animal basis, there was no significant 2-way interaction between genotype and sound level for either female rats or male rats, as well as no main effect of genotype for either females (F(1, 9) = 1.597, $P = 0.2381$; Fig. 5A) or males (F(1, 10) = 0.303, $P = 0.5940$; Fig. 5B). Thus, there were modest differences in the normalized curves at the multiunit level and these differences between the genotypes did not hold when analyzed per animal. However, when comparing

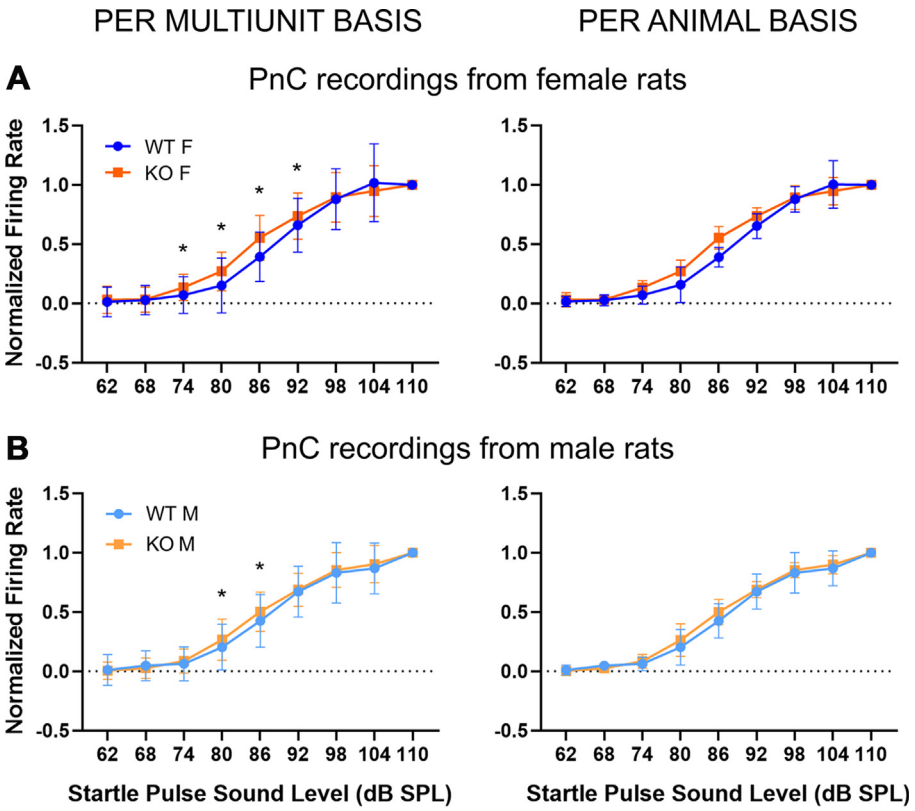

Fig. 5. Normalized firing rates show that *Cntnap2*$^{-/-}$ PnC curves are modestly leftward-shifted compared with PnC curves from wildtype rats. **(A)** On a multiunit basis, normalized firing rates in the PnC were significantly higher in *Cntnap2*$^{-/-}$ females at moderate sound levels ($P < 0.05$) compared with wildtype females. On an animal basis, there were no significant differences between the genotypes for normalized PnC firing rates in female rats. **(B)** On a multiunit basis, normalized firing rates in the PnC were significantly higher in *Cntnap2*$^{-/-}$ males at moderate sound levels ($P < 0.05$) compared with wildtype males. On an animal basis, there were no significant differences between the genotypes for normalized PnC firing rates in male rats. Females: $N = 177$ multiunits from 6 wildtypes, 157 multiunits from 5 knock-outs. Males: $N = 192$ multiunits from 6 wildtypes, 188 multiunits from 6 knock-outs. Graphs show mean ± SD. *$P < 0.05$.

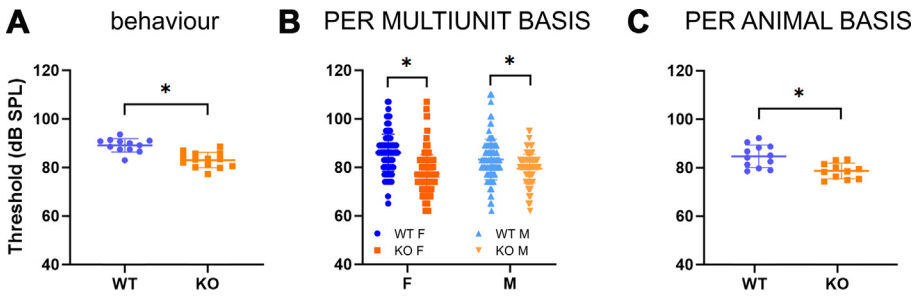

Fig. 6. Lower startle thresholds in *Cntnap2*$^{-/-}$ rats was accompanied by lower PnC activation thresholds. **(A)** *Cntnap2*$^{-/-}$ rats showed significantly lower startle thresholds ($P < 0.05$) compared with wildtype rats. **(B)** On a multiunit basis, *Cntnap2*$^{-/-}$ multiunits showed significantly lower PnC firing rate thresholds compared with wildtype multiunits, for both females and males ($P < 0.05$). **(C)** On an animal basis, *Cntnap2*$^{-/-}$ rats showed significantly lower PnC firing rate thresholds compared with wildtype rats. Wildtype: $N = 12$ rats; PnC = 177 multiunits from 6 females, 192 multiunits from 6 males. *Cntnap2*$^{-/-}$: $N = 14$ rats; PnC = 157 multiunits from 5 females, 188 multiunits from 6 males. Graphs show mean ± SD. *$P < 0.05$.

thresholds between wildtype and *Cntnap2*$^{-/-}$ rats, it indicates that the *Cntnap2*$^{-/-}$ curves are indeed leftward-shifted relative to wildtype curves. For the multiunit analysis, there was a significant 2-way interaction between sex and genotype ($F(1, 710) = 18.48$, $P < 0.0001$) and post-hoc tests revealed that *Cntnap2*$^{-/-}$ multiunits had lower PnC activation thresholds than wildtype multiunits for both females ($P < 0.0001$) and males ($P < 0.0001$; Fig. 6B). On a per animal basis, there was no significant 2-way interaction. Collapsing across sex, *Cntnap2*$^{-/-}$ rats showed significantly lower PnC activation thresholds than wildtypes (main effect of genotype: $F(1, 19) = 13.73$, $P = 0.0015$; Fig. 6C). Lower PnC activation thresholds in *Cntnap2*$^{-/-}$ rats parallels lower startle thresholds in *Cntnap2*$^{-/-}$ rats compared with wildtypes (main effect of genotype: $F(1, 22) = 25.12$, $P < 0.0001$; Fig. 6A).

To assess if the marked increase in firing rates in the PnC of female *Cntnap2*$^{-/-}$ rats persists across multiple brain regions, PPTg firing rates in response to startle pulses were analyzed. For the multiunit analysis, there was a significant 3-way interaction between sex × genotype × sound level ($F(8, 5544) = 4.262$, $P < 0.0001$; Fig. 7A). For females, there was a significant 2-way interaction between genotype and sound level ($F(8, 2496) = 8.790$, $P < 0.0001$) and post-hoc tests revealed that *Cntnap2*$^{-/-}$ females had increased PPTg firing rates compared with wildtype females at 110 dB SPL ($P < 0.05$; Fig. 7B). For males, there was also a significant 2-way interaction between genotype and sound level ($F(8, 3048) = 2.087$, $P = 0.0338$) and post-hoc tests revealed significantly increased PPTg firing rates in *Cntnap2*$^{-/-}$ males compared with wildtype males at 62 and 74 dB SPL ($P < 0.05$; Fig. 7C). However, at the animal level, there were no interactions involving genotype and no significant differences between the genotypes for PPTg firing rates (main effect of genotype: $F(1, 18) = 0.133$, $P = 0.720$; Fig. 7A). There were no subsequent analyses run for female and male rats separately, but the respective graphs are still shown in panels B and C of Fig. 7 to serve as a visual comparison alongside the multiunit female and male graphs. Overall, the differences between the genotypes for PPTg firing rates were very subtle at the multiunit level and did not persist at the animal level. Thus, the large difference between the genotypes in females and the sex differential effects of a loss of function mutation in the *Cntnap2* gene that were observed in the PnC are absent in the PPTg.

Looking at properties beyond the firing rate, response onset latency and response duration of sound-evoked activity in the PnC were compared between wildtype and *Cntnap2*$^{-/-}$ rats. Response onset was defined as the time point at which firing rate was significantly and consistently above spontaneous activity levels. Response offset was defined as the time point at which firing rate returned to spontaneous activity levels. Response duration was calculated as response onset subtracted from response offset. For multiunit analysis of response onset latencies, there was a significant 3-way interaction (sex × genotype × sound level interaction: $F(5, 2914) = 2.459$, $P = 0.0312$; Supplementary Fig. 3A). For females, there was a significant 2-way interaction between genotype and sound level ($F(5, 1311) = 4.838$, $P = 0.0002$) and post-hoc tests showed that *Cntnap2*$^{-/-}$ females have significantly shorter PnC response onset latencies than wildtype females at 92, 98, and 110 dB SPL ($P < 0.05$; Supplementary Fig. 3B). For males, there was also a significant 2-way interaction between genotype and sound level ($F(5, 1603) = 2.602$, $P = 0.0237$) and post-hoc tests showed that *Cntnap2*$^{-/-}$ males have shorter PnC response onset latencies than wildtype males at 98 and 104 dB SPL ($P < 0.05$; Supplementary Fig. 3C). On a per animal basis, there was no significant 3-way interaction for response onset latencies but there was a significant 2-way interaction between genotype and sound level ($F(5, 93) = 3.819$, $P = 0.003$). Collapsed across sex, post-hoc tests showed that *Cntnap2*$^{-/-}$ rats have significantly shorter PnC response onset latencies at 98 dB SPL ($P = 0.046$) compared with wildtype rats (Supplementary Fig. 3E).

For multiunit analysis of response duration times, there was a significant 3-way interaction between sex × genotype × sound level ($F(5, 2914) = 4.370$, $P = 0.0006$; Supplementary Fig. 4A). There was a significant 2-way interaction between genotype and sound level for females ($F(5, 1311) = 4.807$, $P = 0.0002$) and post-hoc tests showed that *Cntnap2*$^{-/-}$ females have significantly longer response duration times than wildtype females at 86, 92, and 98 dB SPL ($P < 0.05$; Supplementary Fig. 4B). Males also had a significant 2-way interaction between genotype and sound level ($F(5, 1603) = 2.524$, $P = 0.0276$), but no significant differences were found at specific sound levels (Supplementary Fig. 4C).

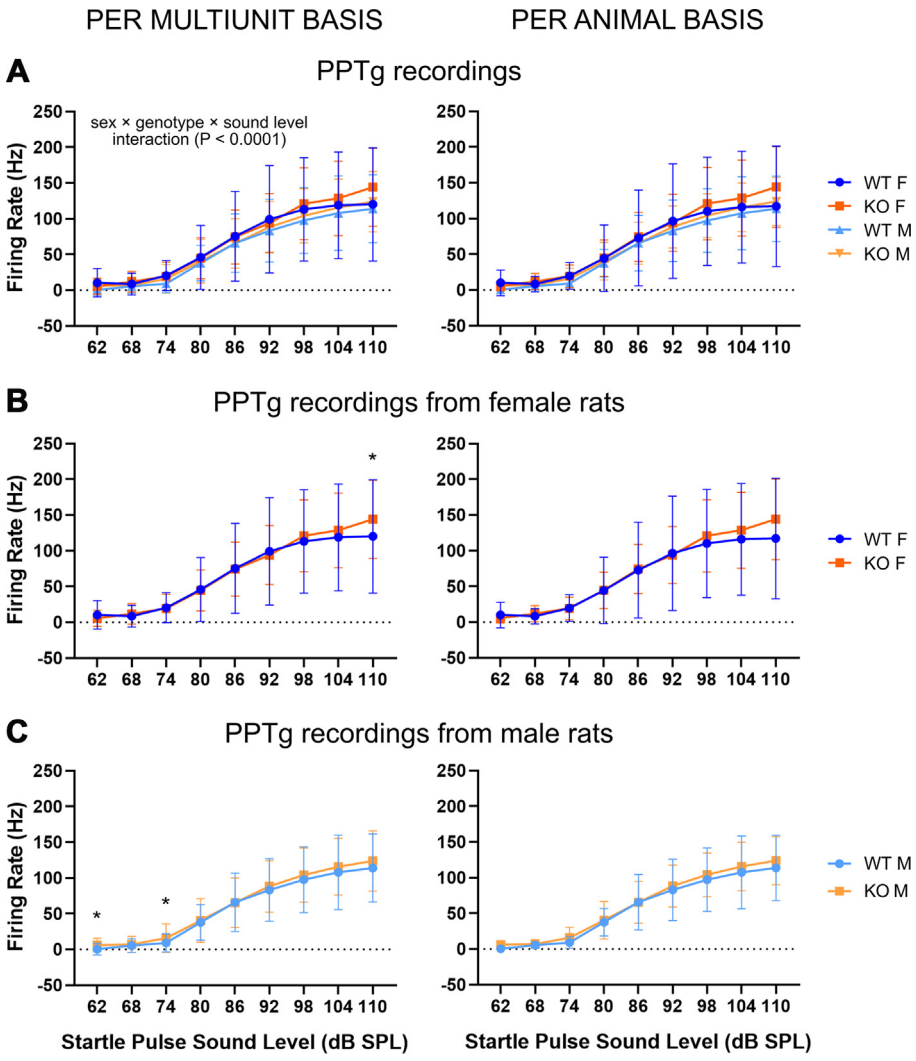

Fig. 7. The marked increase in PnC firing rates in female *Cntnap2*$^{-/-}$ rats was not observed for PPTg firing rates. **(A)** At the multiunit level, a significant 3-way interaction was found for sex × genotype × sound level. At the animal level, there were no interactions involving genotype and no main effect of genotype. **(B)** Firing rates in the PPTg were increased in *Cntnap2*$^{-/-}$ females ($P < 0.05$) at 110 dB SPL compared with wildtype females when analyzed on a multiunit basis. Although no statistics were run on an animal basis for females alone, the per animal graph is shown on the right for comparison. **(C)** Firing rates in the PPTg were increased in *Cntnap2*$^{-/-}$ males ($P < 0.05$) at low sound levels compared with wildtype males when analyzed on a multiunit basis. Although no statistics were run on an animal basis for males alone, the per animal graph is shown on the right for comparison. Wildtype: PPTg = 154 multiunits from 5 females, 159 multiunits from 5 males. *Cntnap2*$^{-/-}$: PPTg = 160 multiunits from 5 females, 224 multiunits from 7 males. Graphs show mean ± SD. *$P < 0.05$.

These findings further reinforce the sex-specific effects of a loss of function mutation in the *Cntnap2* gene. For the per animal analysis, there were no significant interactions involving genotype or main effects of genotype for response duration times (main effect of genotype: F(1, 19) = 2.622, P = 0.1219; Supplementary Fig. 4A). Although there was no subsequent per animal analysis run for female rats and male rats separately, the respective graphs are still shown in panels B and C of Supplementary Fig. 4 to serve as a visual comparison alongside the multiunit female and male graphs.

PPI

Sensorimotor gating was assessed through a prepulse inhibition (PPI) paradigm. PPI was measured by presenting 20 trials of 20-ms, 105 dB SPL startle pulses preceded by 10-ms prepulses ranging from 65 to 89 dB SPL, in 6 dB steps. Consistent with previous reports, *Cntnap2*$^{-/-}$ rats showed decreased %PPI compared with wildtypes (main effect of genotype: F(1, 22) = 21.84, P = 0.0001; Fig. 8A). As expected, PnC firing rates in response to the startle stimulus decreased when the startle stimulus was preceded by a prepulse (Fig. 3B). However, the differences between the genotypes for % reduction in PnC firing rates was in the opposite direction as behavioural %PPI. For multiunit analysis, there was a significant 3-way interaction (sex × genotype × sound level interaction: F(4, 2812) = 11.46, $P < 0.0001$; Fig. 8B). Females had a significant 2-way interaction between genotype and sound level (F(4, 1304) = 4.691, P = 0.0009) and post-hoc tests revealed that *Cntnap2*$^{-/-}$ females had increased % reduction in PnC firing rates compared with wildtype females when startle pulses were preceded by 83 dB SPL prepulses (P = 0.0019; Fig. 8C). Males also had a significant 2-way interaction between genotype and sound level (F(4, 1508) = 14.35, $P < 0.0001$) and post-hoc tests revealed that *Cntnap2*$^{-/-}$ males had increased % reduction in PnC firing rates compared with wildtype males when startle pulses were preceded by 65 dB SPL prepulses ($P < 0.0001$; Fig. 8D). These results indicate that decreased % PPI in *Cntnap2*$^{-/-}$ rats is not explained by decreased % reduction in PnC firing rates. This is reinforced by the per animal analysis, in which there were no significant interactions involving genotype and no significant main effect of genotype (main effect of genotype: F(1, 19) = 0.07992, P = 0.7805; Fig. 8B). Although there was no subsequent analysis run for female rats and male rats separately, the respective per animal graphs are shown in panels B and C of Fig. 8 to serve as a visual comparison alongside the multiunit female and male graphs. Additionally, firing rates in the PPTg in response to the 10-ms prepulses alone were not

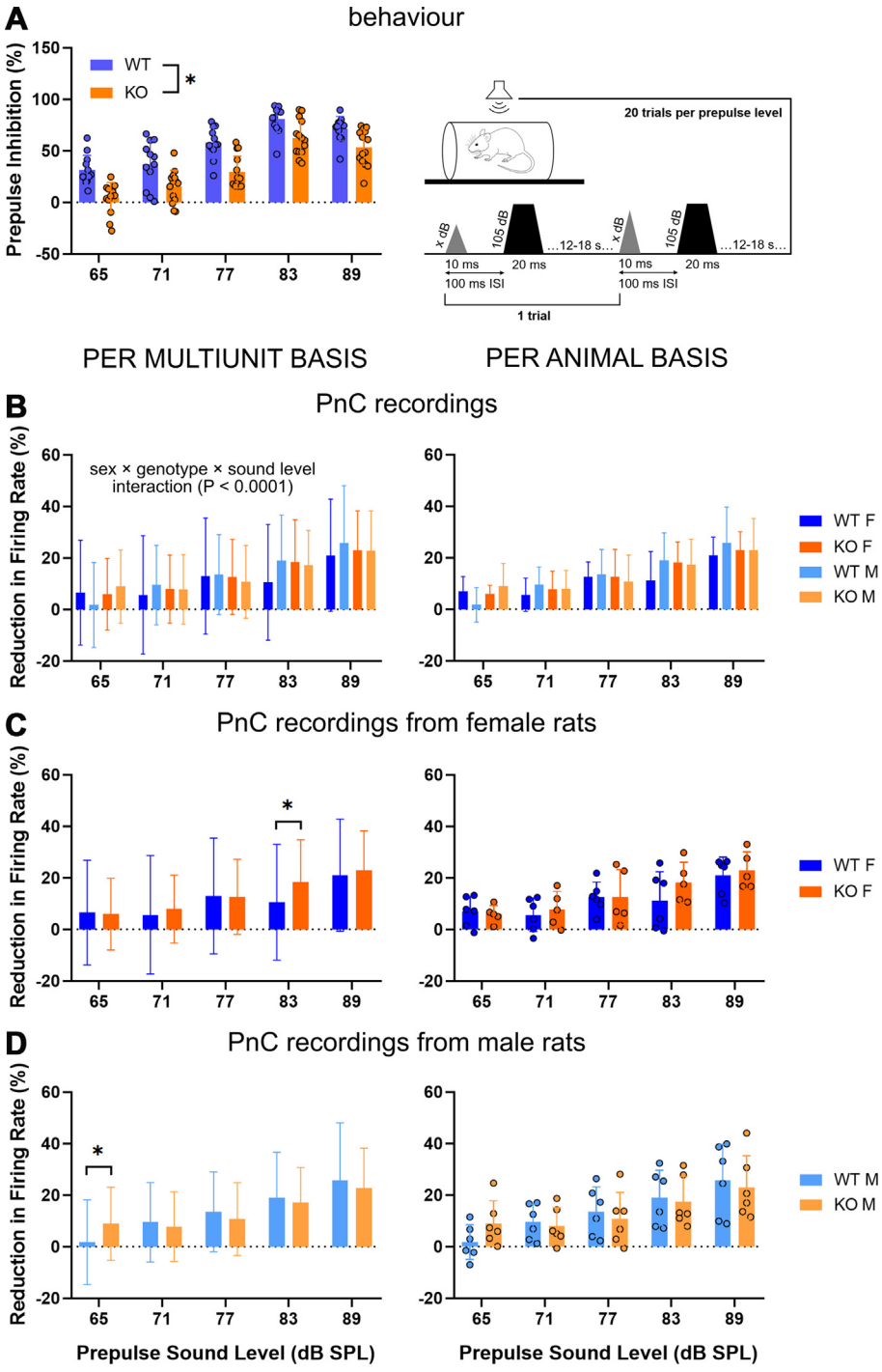

Fig. 8. Decreased PPI in *Cntnap2*$^{-/-}$ rats compared with wildtype rats was not accompanied by decreased reduction of PnC firing rates. **(A)** Acoustic startle stimuli at 105 dB SPL were preceded by prepulses ranging from 65 to 89 dB SPL, in 6 dB steps, or no prepulse (i.e., 0 dB "prepulse"). Each prepulse sound level, including no prepulse, was presented 20 times with 12–18 second inter-trial intervals. *Cntnap2*$^{-/-}$ rats showed significantly decreased %PPI ($P < 0.05$). **(B)** On a multiunit basis, there was a significant 3-way interaction between sex × genotype × sound level. On an animal basis, there were no significant interactions involving genotype and no significant main effect of genotype. **(C)** At the multiunit level, *Cntnap2*$^{-/-}$ females had significantly increased % reduction in PnC firing rates in the 83 dB SPL prepulse condition ($P < 0.05$) compared with wildtype females. Although no statistics were run on a per animal basis for female rats alone, the graph is shown on the right for comparison. **(D)** At the multiunit level, *Cntnap2*$^{-/-}$ males had significantly increased % reduction in PnC firing rates in the 65 dB SPL prepulse condition ($P < 0.05$) compared with wildtype males. Although no statistics were run on a per animal basis for male rats alone, the graph is shown on the right for comparison. Wildtype: $N = 12$ rats; PnC = 173 multiunits from 6 females, 191 multiunits from 6 males. *Cntnap2*$^{-/-}$: $N = 14$ rats; PnC = 155 multiunits from 5 females, 188 multiunits from 6 males. Graphs show mean ± SD. *$P < 0.05$.

significantly different between wildtype rats and *Cntnap2*$^{-/-}$ rats, for either multiunits (genotype × sound level interaction: $F(4, 2772) = 3.969$, $P = 0.0032$, no significant differences at specific sound levels; Fig. 9A) or animals (main effect of genotype: $F(1, 18) < 0.0001$, $P = 0.9965$; Fig. 9B). Thus, *Cntnap2*$^{-/-}$ rats do not have altered inhibition of the PnC by prepulse-evoked PPTg activity.

DISCUSSION

The present study aimed to investigate the electrical activity of brainstem structures in the ASR and PPI neural pathways in rats with and without a loss of function mutation in the *Cntnap2* gene. Auditory brainstem responses and electrophysiological recordings conducted in the PnC and PPTg, as well as behavioural startle experiments, were performed in the same rats to determine whether or not altered sound-evoked activity in the PnC and PPTg contributes to *Cntnap2*-related changes in acoustic startle reactivity and sensorimotor gating. Consistent with previous literature (Scott et al., 2018; 2020; Möhrle et al., 2021), adult *Cntnap2*$^{-/-}$ rats showed increased ASR, lower ASR thresholds, and decreased PPI compared with wildtype rats, while their ABRs were not different. This indicates that *Cntnap2*$^{-/-}$ rats are not more sensitive to sound at the level of the cochlea or downstream auditory processing pathways in the brainstem, as this would have led to changes in the early waves of the ABR. We therefore focused on the PnC and PPTg, and found that *Cntnap2*$^{-/-}$ rats showed increased PnC responsivity compared with wildtypes. This increase was marked in female *Cntnap2*$^{-/-}$ rats but modest in male *Cntnap2*$^{-/-}$ rats. There were minimal differences between the genotypes for PPTg responsivity, which aligned with the finding of minimal differences between the genotypes for PnC inhibition during a PPI paradigm.

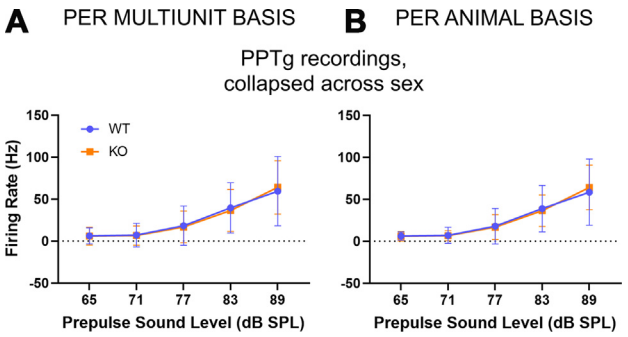

Fig. 9. The amount of inhibition on the PnC by prepulse-evoked PPTg activity was not different between wildtype and *Cntnap2*$^{-/-}$ rats. **(A)** For the per multiunit analysis, there were no significant differences between the genotypes for PPTg firing rates in response to the prepulses alone. **(B)** For the per animal analysis, there were no significant differences between the genotypes for PPTg firing rates in response to the prepulses alone. Wildtype: PPTg = 154 multiunits from 5 females, 159 multiunits from 5 males. *Cntnap2*$^{-/-}$: PPTg = 160 multiunits from 5 females, 224 multiunits from 7 males. Graphs show mean ± SD. *P < 0.05.

Electrophysiological validity

As shown in Fig. 4, startle magnitudes increased with increasing startle pulse sound level, and this was paralleled by increasing PnC and PPTg firing rates. PnC onset latencies decreased with increasing sound level (Supplementary Fig. 3) and PnC durations of activity increased slightly with increasing sound level (Supplementary Fig. 4), both of which reflect increased responsivity in response to louder acoustic stimuli. PPI was paralleled by a respective reduction in PnC firing rates. This reduction of PnC firing rates also grew larger with increasing prepulse sound level, indicating that there is more inhibition of PnC activity with louder prepulses (Fig. 8). Collectively, these data validate the PnC as a site of sound-evoked pre-motor activity, as proposed by multiple studies (Lingenhöhl and Friauf, 1992, 1994; Weber et al., 2002; Simons-Weidenmaier et al., 2006; Zaman et al., 2017). Additionally, PPTg firing rates increased with increasing prepulse sound level, which supports the proposed PPI pathway whereby sound-sensitive PPTg neurons inhibit the PnC startle-mediating neurons, leading to more inhibition from the PPTg to the PnC with louder prepulses (Swerdlow and Geyer, 1993; Yeomans et al., 2006; MacLaren et al., 2014; Azzopardi et al., 2018; Fulcher et al., 2020). Thus, the measures obtained from the electrophysiological recordings conducted in the PnC and PPTg in response to a range of startle pulse and prepulse sound levels correlated well with the behavioural outputs and validated the proposed startle and PPI circuits.

Neural basis of increased startle

As expected, there was increased ASR excitability in *Cntnap2*$^{-/-}$ rats compared with wildtype rats. Startle magnitudes were significantly increased for *Cntnap2*$^{-/-}$ rats at moderate sound levels and ASR thresholds were significantly lower, meaning that *Cntnap2*$^{-/-}$ rats began startling at quieter sound intensities compared with wildtype rats. PnC firing rates were increased, PnC activation thresholds were lower, PnC response onset latencies were shorter, and PnC response duration times were longer in *Cntnap2*$^{-/-}$ rats, all of which indicate increased responsiveness of the PnC in *Cntnap2*$^{-/-}$ rats. However, there was a sex difference as these changes were more considerable in female *Cntnap2*$^{-/-}$ rats and modest or absent in male *Cntnap2*$^{-/-}$ rats, even though both female and male *Cntnap2*$^{-/-}$ rats have similarly increased ASR excitability compared with wildtype rats. Thus, it seems that a loss of function mutation in the *Cntnap2* gene partially affects ASR through increased firing rates in auditory-responsive PnC neurons, presumably the startle mediating pre-motor neurons (Lingenhöhl and Friauf, 1992, 1994), which would in turn increase activation of motor neurons to elicit the startle response. Molecularly, increased PnC responsiveness may be due to increased presynaptic neurotransmitter release (Scott et al., 2019) or increased frequency of synaptic input to *Cntnap2*$^{-/-}$ neurons (unpublished data). A recent study from our lab has shown that there are no differences in intrinsic excitability between neurons from adult *Cntnap2*$^{-/-}$ rats and wildtype littermates (unpublished data). However, there is altered synaptic input in auditory cortex pyramidal neurons of adult *Cntnap2*$^{-/-}$ rats, specifically, more frequent spontaneous excitatory post-synaptic currents and mini excitatory post-synaptic currents compared with wildtype rats (unpublished data). A similar change could potentially be happening in the brainstem, although future *in vitro* recordings are needed to confirm this. In contrast, in homozygously-bred *Cntnap2*$^{-/-}$ rats, there were no differences in synaptic inputs between wildtype and *Cntnap2*$^{-/-}$ rats, but *Cntnap2*$^{-/-}$ cells were more intrinsically excitable than wildtype cells (Scott et al., 2022), highlighting the importance of parental genotype.

Male *Cntnap2*$^{-/-}$ rats only had modestly increased PnC responsiveness compared with male wildtypes. Indeed, PnC firing rates in male wildtypes were generally high, resembling the firing rates in *Cntnap2*$^{-/-}$ rats (Fig. 4B). Furthermore, for female *Cntnap2*$^{-/-}$ rats, the range of startle pulse sound levels at which PnC firing rates were significantly increased did not match the startle pulse sound levels at which ASR was significantly increased. Thus, startle magnitude is not solely dependent on neuronal firing rates and there are likely factors other than PnC firing rate that contribute to the neural basis of increased ASR in *Cntnap2*$^{-/-}$ rats, especially in males. A recent study found that homozygous mutations in *CNTNAP2* in brain organoids increased cell proliferation and increased the total cell number (de Jong et al., 2021). A potential explanation is that male *Cntnap2*$^{-/-}$ rats have more PnC giant neurons than male wildtype rats. Increased recruitment of PnC giant neurons to elicit the startle response could contribute to increased startle magnitude. This explanation is also possible for female *Cntnap2*$^{-/-}$ rats, which may have increased number and/or recruitment of PnC giant neurons along with markedly increased PnC firing rates.

An alternative explanation for increased ASR in *Cntnap2*$^{-/-}$ rats is that there is a brain region that mediates ASR in rats other than the PnC, and that this region is altered in *Cntnap2*$^{-/-}$ rats, resulting in increased startle. It is generally accepted that the PnC is the primary brainstem structure that mediates ASR (Lingenhöhl and Friauf, 1992, 1994). However, a recent paper by Guo et al. (2021) concluded that the reticulotegmental nucleus (RtTg) can also mediate ASR. Using mice, the authors observed that startle responses were induced by optogenetic activation of RtTg neurons and ASR magnitude was decreased by chemogenetic inhibition of RtTg glutamatergic neurons (Guo et al., 2021). Additionally, the mean spike latency of RtTg neurons was approximately 5.12 ms in response to acoustic stimuli (Guo et al., 2021), which is a short enough latency to mediate the ASR. Finally, the authors found that the RtTg is innervated by neurons in the CN and that RtTg neurons project directly to spinal cord motor neurons (Guo et al., 2021). Thus, if the RtTg mediates acoustic startle, altered RtTg responsivity may underly increased ASR in *Cntnap2*$^{-/-}$ rats. However, future studies are needed to confirm the RtTg as a brain region that mediates ASR and to further investigate specifically which neurons in the RtTg mediate ASR. It would also be of interest to look at sex-dependent differences in the RtTg, especially in animal models of ASD such as *Cntnap2*$^{-/-}$ rats.

PPTg firing rates in response to startle pulses were significantly different between wildtype and *Cntnap2*$^{-/-}$ rats at very few sound levels, and only when analyzed on a per multiunit basis. Thus, the marked increase in PnC firing rates observed in female *Cntnap2*$^{-/-}$ rats was not due to a generalized large increase in responsivity across multiple brain regions. Various studies have found that *Cntnap2* mutations can either increase, decrease, or not change neuronal activity depending on the brain region of interest. *Cntnap2* mutations led to increased neuronal activity in dorsal root ganglion neurons (Dawes et al., 2018; Xing et al., 2020) and the auditory cortex (Scott et al., 2022), as well as in human induced pluripotent stem cells (Flaherty et al., 2017). On the other hand, there was decreased or unchanged excitatory activity in the hippocampus (Jurgensen and Castillo, 2015), somatosensory cortex (Peñagarikano et al., 2011), primary visual cortex (Bridi et al., 2017), medial prefrontal cortex (Lazaro et al., 2019), suprachiasmatic nucleus (Wang et al., 2020), and cerebellum (Fernández et al., 2021) of *Cntnap2*$^{-/-}$ rats. Overall, these collective results highlight that a loss of function mutation in the *Cntnap2* gene has differential effects depending on the specific brain region.

Finally, normalized PnC firing rates revealed that *Cntnap2*$^{-/-}$ curves are slightly leftward-shifted compared with wildtype curves. However, the differences between the genotypes were inconsistent between the per multiunit and per animal analyses. Additionally, the increase in normalized PnC firing rates was not as drastic as the increase in absolute PnC firing rates for female *Cntnap2*$^{-/-}$ rats compared with female wildtypes. These results indicate that female *Cntnap2*$^{-/-}$ rats have a much higher maximum PnC firing rate than female wildtypes, but there are modest differences between the genotypes in terms of the ratio at which PnC firing rates increase as startle pulses get louder. For behavioural ASR, absolute values show if there is a change in the startle response itself, whereas normalized values show if there is a change in sound processing (Miller et al., 2021). The respective absolute versus normalized PnC firing rates could similarly reflect different components of sensory processing at the neuronal level.

Overall, altered PnC electrical activity cannot fully explain increased reactivity to acoustic stimuli in *Cntnap2*$^{-/-}$ rats considering that PnC differences between the genotypes were more drastic in female rats than in male rats, whereas increased ASR in *Cntnap2*$^{-/-}$ rats is not sex-differential. Thus, there are likely other factors beyond PnC responsivity that contribute to increased ASR excitability in *Cntnap2*$^{-/-}$ rats. Future studies could investigate potential differences in the number of PnC giant neurons, morphology of PnC giant neurons, PnC giant neuron recruitment in response to acoustic stimuli, and other brain regions that may mediate ASR. Any combination of these factors could contribute to the hyper-reactivity to sound observed in *Cntnap2*$^{-/-}$ rats.

Neural basis of impaired sensorimotor gating

Consistent with previous studies (Möhrle et al., 2021; Scott et al., 2018, 2020), *Cntnap2*$^{-/-}$ rats showed significantly decreased %PPI compared with wildtype rats. During PPI, the decrease in ASR magnitude is presumably due to PnC activity being inhibited by PPTg activity (Koch, 1999). Surprisingly, *Cntnap2*$^{-/-}$ rats had increased inhibition of PnC firing rates compared with wildtype rats at specific prepulse sound levels, which is in the opposite direction of the behavioural results. Furthermore, there were no significant differences between the genotypes for PPTg firing rates in response to the prepulses alone, indicating that inhibition of the PnC by PPTg activity was the same between wildtype and *Cntnap2*$^{-/-}$ rats. This raises the question: what is causing decreased PPI in *Cntnap2*$^{-/-}$ rats if not decreased inhibition by the PPTg, and subsequent decreased reduction in PnC firing rates? It is important to acknowledge that there are many brain structures other than the PPTg that modulate the primary ASR pathway, such as the locus coeruleus, inferior colliculus, and superior colliculus (Fendt et al., 2001; Hormigo et al., 2015; Gómez-Nieto et al., 2020). These brain regions may have altered activity in *Cntnap2*$^{-/-}$ rats, affecting PPI. However, whether it be through a direct or indirect projection, these secondary structures must still ultimately impact PnC activity to modulate the acoustic startle response (Fendt et al., 2001; Gómez-Nieto et al., 2020). Thus, if *Cntnap2*$^{-/-}$ rats do not have altered PnC inhibition in terms of % reduction in firing rates, decreased PPI in *Cntnap2*$^{-/-}$ rats is unlikely to be explained by altered inhibition from these other brain regions that modulate ASR.

Another consideration is that the field generally assumes that PPI is independent of baseline startle.

However, Csomor et al. (2008) argued that PPI magnitude depends on baseline startle regardless of how PPI is calculated. Thus, considering that *Cntnap2*$^{-/-}$ rats have elevated baseline ASR, the differences between the genotypes for PPI could potentially be attributed to differences in baseline startle rather than neural changes. Alternatively, PPI differences between the genotypes may be caused by the effects of loss of CASPR2 expression that are even further downstream in the ASR pathway than the PnC, such as at the level of motor neurons. CASPR2 has been found to be present in myelinated axons of various nerves in mice (Poliak et al., 1999, 2001), so loss of CASPR2 expression in motor neurons could potentially contribute to PPI deficits in *Cntnap2*$^{-/-}$ rats. Future studies could investigate if there are *Cntnap2*-related alterations in motor neuron electrical activity or potential differences in PnC giant neuron innervation of motor neurons.

Limitations

A limitation of this study is that we do not know if the recorded PnC activity is from PnC giant neurons or from other PnC neurons that respond to sound (Koch et al., 1992). Future *in vitro* electrophysiological studies could investigate the specific impact of a loss of function mutation in the *Cntnap2* gene on the electrical activity of visually identified startle-mediating PnC giant neurons. Another limitation of this study is that the experiments were only conducted in adult rats, but is it known that a loss of function mutation in the *Cntnap2* gene has varying effects depending on rat age (Scott et al., 2018). Future studies could include *Cntnap2*$^{-/-}$ rats across different stages of development to gain a better understanding of the neural changes that occur with a loss of function mutation in the *Cntnap2* gene. Finally, the sex differences for PnC responsivity may be due to variabilities in sensitivity to anesthesia. A study by Zambricki and Dalecy (2004) found that male rats had lower plasma concentrations of the anesthetic sodium pentobarbital compared with female rats. There is little literature on sex differences with regards to the doses of ketamine/xylazine used to induce deep anesthesia in rats, but this possibility cannot be excluded.

In sum, this study investigated brainstem structures important in mediating the acoustic startle response and prepulse inhibition, and compared the neural activity between *Cntnap2*$^{-/-}$ rats and wildtype littermates. Electrophysiological recordings were successful as evidenced by how the various measures obtained from the PnC and PPTg correlated well with their respective behavioural outputs. Although our findings confirm neural correlates for ASR and PPI in the PnC and PPTg, some results warrant further research into the specific properties of those brain regions that could affect startle magnitude and %PPI values. We revealed that (1) increased ASR excitability in rats with a functional loss of *Cntnap2* is associated with increased PnC responsiveness, but inconsistently so in male *Cntnap2*$^{-/-}$ rats, and (2) decreased PPI in *Cntnap2*$^{-/-}$ rats is not associated with decreased inhibition of PnC firing rates or with altered PPTg responsiveness. These findings suggest that there are other mechanisms that contribute to altered auditory processing observed in *Cntnap2*$^{-/-}$ rats beyond PnC and PPTg electrical activity, and there are numerous potential alternative mechanisms that can be explored. Future studies will investigate other properties of the PnC and PPTg in *Cntnap2*$^{-/-}$ rats, such as neuron recruitment and neuronal morphology, as well as investigate additional structures in the ASR and PPI pathways to better understand how a loss of function mutation in the *Cntnap2* gene impacts auditory processing.

ACKNOWLEDGEMENTS

This work was funded by the Canadian Institutes of Health Research (CIHR) project grant to SS and BLA, and by the Natural Sciences and Engineering Council of Canada (NSERC) Discovery grant to SS.

AZ analysed all data, drafted the manuscript, and made all figures, KES performed the experiments and helped with data analysis, ALS helped with data analysis, RM helped with experiments, BLA was involved with conceptional design of the study, data analysis and manuscript review, and SS was involved with conceptional design of the study, data analysis, manuscript review and handling of manuscript.

APPENDIX A. SUPPLEMENTARY MATERIAL

Supplementary material to this article can be found online at https://doi.org/10.1016/j.neuroscience.2023.01.020.

REFERENCES

Anderson GR, Galfin T, Xu W, Aoto J, Malenka RC, Südhof TC (2012) Candidate autism gene screen identifies critical role for cell-adhesion molecule CASPR2 in dendritic arborization and spine development. Proc Natl Acad Sci U S A 109:18120–18125. https://doi.org/10.1073/pnas.1216398109.

Azzopardi E, Louttit AG, DeOliveira C, Laviolette SR, Schmid S (2018) The Role of Cholinergic Midbrain Neurons in Startle and Prepulse Inhibition. J Neurosci 38:8798–8808. https://doi.org/10.1523/JNEUROSCI.0984-18.2018.

Bridi MS, Park SM, Huang S (2017) Developmental Disruption of GABAAR-Meditated Inhibition in Cntnap2 KO Mice. eNeuro 4. https://doi.org/10.1523/ENEURO.0162-17.2017. ENEURO.0162-17.2017.

Cheng C-H, Chan P-Y-S, Hsu S-C, Liu C-Y (2018) Meta-analysis of sensorimotor gating in patients with autism spectrum disorders. Psychiatry Res 262:413–419. https://doi.org/10.1016/j.psychres.2017.09.016.

Csomor PA, Yee BK, Vollenweider FX, Feldon J, Nicolet T, Quednow BB (2008) On the influence of baseline startle reactivity on the indexation of prepulse inhibition. Behav Neurosci 122:885–900. https://doi.org/10.1037/0735-7044.122.4.885.

Dawes JM, Weir GA, Middleton SJ, Patel R, Chisholm KI, Pettingill P, Peck LJ, Sheridan J, Shakir A, Jacobson L, Gutierrez-Mecinas M, Galino J, Walcher J, Kühnemund J, Kuehn H, Sanna MD, Lang B, Clark AJ, Themistocleous AC, Iwagaki N, West SJ, Werynska K, Carroll L, Trendafilova T, Menassa DA, Giannoccaro MP, Coutinho E, Cervellini I, Tewari D, Buckley C, Leite MI, Wildner H, Zeilhofer HU, Peles E, Todd AJ, McMahon SB, Dickenson AH, Lewin GR, Vincent A, Bennett DL (2018) Immune or Genetic-Mediated Disruption of CASPR2 Causes Pain Hypersensitivity Due to Enhanced Primary Afferent Excitability. Neuron 97:806–822.e10. https://doi.org/10.1016/j.neuron.2018.01.033.

de Jong JO, Llapashtica C, Genestine M, Strauss K, Provenzano F, Sun Y, Zhu H, Cortese GP, Brundu F, Brigatti KW, Corneo B, Migliori B, Tomer R, Kushner SA, Kellendonk C, Javitch JA, Xu B, Markx S (2021) Cortical overgrowth in a preclinical forebrain organoid model of CNTNAP2-associated autism spectrum disorder. Nat Commun 12:4087. https://doi.org/10.1038/s41467-021-24358-4.

Erturk O, Korkmaz B, Alev G, Demirbilek V, Kiziltan M (2016) Startle and blink reflex in high functioning autism. Neurophysiol Clin 46:189–192. https://doi.org/10.1016/j.neucli.2016.02.001.

Fendt M, Li L, Yeomans JS (2001) Brain stem circuits mediating prepulse inhibition of the startle reflex. Psychopharmacology (Berl) 156:216–224. https://doi.org/10.1007/s002130100794.

Fernández M, Sánchez-León CA, Llorente J, Sierra-Arregui T, Knafo S, Márquez-Ruiz J, Peñagarikano O (2021) Altered Cerebellar Response to Somatosensory Stimuli in the Cntnap2 Mouse Model of Autism. eNeuro 8. https://doi.org/10.1523/ENEURO.0333-21.2021. ENEURO.0333-21.2021.

Flaherty E, Deranieh RM, Artimovich E, Lee IS, Siegel AJ, Levy DL, Nestor MW, Brennand KJ (2017) Patient-derived hiPSC neurons with heterozygous CNTNAP2 deletions display altered neuronal gene expression and network activity. NPJ Schizophr 3:35. https://doi.org/10.1038/s41537-017-0033-5.

Fulcher N, Azzopardi E, De Oliveira C, Hudson R, Schormans AL, Zaman T, Allman BL, Laviolette SR, Schmid S (2020) Deciphering midbrain mechanisms underlying prepulse inhibition of startle. Prog Neurobiol 185. https://doi.org/10.1016/j.pneurobio.2019.101734 101734.

Gómez-Nieto R, Hormigo S, López DE (2020) Prepulse Inhibition of the Auditory Startle Reflex Assessment as a Hallmark of Brainstem Sensorimotor Gating Mechanisms. Brain Sci 10:639. https://doi.org/10.3390/brainsci10090639.

Gordon A, Salomon D, Barak N, Pen Y, Tsoory M, Kimchi T, Peles E (2016) Expression of Cntnap2 (Caspr2) in multiple levels of sensory systems. Mol Cell Neurosci 70:42–53. https://doi.org/10.1016/j.mcn.2015.11.012.

Guo W, Fan S, Xiao D, Dong H, Xu G, Wan Z, Ma Y, Wang Z, Xue T, Zhou Y, Li Y, Xiong W (2021) A Brainstem reticulotegmental neural ensemble drives acoustic startle reflexes. Nat Commun 12:6403. https://doi.org/10.1038/s41467-021-26723-9.

Hormigo S, Gómez-Nieto R, Castellano O, Herrero-Turrión MJ, López DE, de Anchieta de Castro e Horta-Júnior J (2015) The noradrenergic projection from the locus coeruleus to the cochlear root neurons in rats. Brain Struct Funct 220:1477–1496. https://doi.org/10.1007/s00429-014-0739-3.

Jurgensen S, Castillo PE (2015) Selective Dysregulation of Hippocampal Inhibition in the Mouse Lacking Autism Candidate Gene CNTNAP2. J Neurosci 35:14681–14687. https://doi.org/10.1523/JNEUROSCI.1666-15.2015.

Koch M (1999) The neurobiology of startle. Prog Neurobiol 59:107–128. https://doi.org/10.1016/s0301-0082(98)00098-7.

Koch M, Lingenhöhl K, Pilz PK (1992) Loss of the acoustic startle response following neurotoxic lesions of the caudal pontine reticular formation: possible role of giant neurons. Neuroscience 49:617–625. https://doi.org/10.1016/0306-4522(92)90231-p.

Lazaro MT, Taxidis J, Shuman T, Bachmutsky I, Ikrar T, Santos R, Marcello GM, Mylavarapu A, Chandra S, Foreman A, Goli R, Tran D, Sharma N, Azhdam M, Dong H, Choe KY, Peñagarikano O, Masmanidis SC, Rácz B, Xu X, Geschwind DH, Golshani P (2019) Reduced Prefrontal Synaptic Connectivity and Disturbed Oscillatory Population Dynamics in the CNTNAP2 Model of Autism. Cell Rep 27:2567–2578.e6. https://doi.org/10.1016/j.celrep.2019.05.006.

Lee Y, López DE, Meloni EG, Davis M (1996) A primary acoustic startle pathway: obligatory role of cochlear root neurons and the nucleus reticularis pontis caudalis. J Neurosci 16:3775–3789.

Lingenhöhl K, Friauf E (1992) Giant neurons in the caudal pontine reticular formation receive short latency acoustic input: an intracellular recording and HRP-study in the rat. J Comp Neurol 325:473–492. https://doi.org/10.1002/cne.903250403.

Lingenhöhl K, Friauf E (1994) Giant neurons in the rat reticular formation: a sensorimotor interface in the elementary acoustic startle circuit? J Neurosci 14:1176–1194.

MacLaren DAA, Markovic T, Clark SD (2014) Assessment of sensorimotor gating following selective lesions of cholinergic pedunculopontine neurons. Eur J Neurosci 40:3526–3537. https://doi.org/10.1111/ejn.12716.

Miller EA, Kastner DB, Grzybowski MN, Dwinell MR, Geurts AM, Frank LM (2021) Robust and replicable measurement for prepulse inhibition of the acoustic startle response. Mol Psychiatry 26:1909–1927. https://doi.org/10.1038/s41380-020-0703-y.

Möhrle D, Wang W, Whitehead SN, Schmid S (2021) GABAB Receptor Agonist R-Baclofen Reverses Altered Auditory Reactivity and Filtering in the Cntnap2 Knock-Out Rat. Front Integr Neurosci 15. https://doi.org/10.3389/fnint.2021.710593 710593.

Paxinos, G., Watson, C., 2007. The rat brain in stereotaxic coordinates, 6th ed.

Peñagarikano O, Abrahams BS, Herman EI, Winden KD, Gdalyahu A, Dong H, Sonnenblick LI, Gruver R, Almajano J, Bragin A, Golshani P, Trachtenberg JT, Peles E, Geschwind DH (2011) Absence of CNTNAP2 leads to epilepsy, neuronal migration abnormalities, and core autism-related deficits. Cell 147:235–246. https://doi.org/10.1016/j.cell.2011.08.040.

Poliak S, Gollan L, Martinez R, Custer A, Einheber S, Salzer JL, Trimmer JS, Shrager P, Peles E (1999) Caspr2, a new member of the neurexin superfamily, is localized at the juxtaparanodes of myelinated axons and associates with K+ channels. Neuron 24:1037–1047. https://doi.org/10.1016/s0896-6273(00)81049-1.

Poliak S, Gollan L, Salomon D, Berglund EO, Ohara R, Ranscht B, Peles E (2001) Localization of Caspr2 in myelinated nerves depends on axon-glia interactions and the generation of barriers along the axon. J Neurosci 21:7568–7575.

Rodenas-Cuadrado P, Ho J, Vernes SC (2014) Shining a light on CNTNAP2: complex functions to complex disorders. Eur J Hum Genet 22:171–178. https://doi.org/10.1038/ejhg.2013.100.

Scott KE, Schormans AL, Pacoli KY, De Oliveira C, Allman BL, Schmid S (2018) Altered Auditory Processing, Filtering, and Reactivity in the Cntnap2 Knock-Out Rat Model for Neurodevelopmental Disorders. J Neurosci 38:8588–8604. https://doi.org/10.1523/JNEUROSCI.0759-18.2018.

Scott KE, Kazazian K, Mann RS, Möhrle D, Schormans AL, Schmid S, Allman BL (2020) Loss of Cntnap2 in the Rat Causes Autism-Related Alterations in Social Interactions, Stereotypic Behavior, and Sensory Processing. Autism Res 13:1698–1717. https://doi.org/10.1002/aur.2364.

Scott KE, Mann RS, Schormans AL, Schmid S, Allman BL (2022) Hyperexcitable and Immature-Like Neuronal Activity in the Auditory Cortex of Adult Rats Lacking the Language-Linked CNTNAP2 Gene. Cereb Cortex:bhab517. https://doi.org/10.1093/cercor/bhab517.

Scott R, Sánchez-Aguilera A, van Elst K, Lim L, Dehorter N, Bae SE, Bartolini G, Peles E, Kas MJH, Bruining H, Marín O (2019) Loss of Cntnap2 Causes Axonal Excitability Deficits, Developmental Delay in Cortical Myelination, and Abnormal Stereotyped Motor Behavior. Cereb Cortex 29:586–597. https://doi.org/10.1093/cercor/bhx341.

Simons-Weidenmaier NS, Weber M, Plappert CF, Pilz PKD, Schmid S (2006) Synaptic depression and short-term habituation are located in the sensory part of the mammalian startle pathway. BMC Neurosci 7:38. https://doi.org/10.1186/1471-2202-7-38.

Strauss KA, Puffenberger EG, Huentelman MJ, Gottlieb S, Dobrin SE, Parod JM, Stephan DA, Morton DH (2006) Recessive symptomatic focal epilepsy and mutant contactin-associated protein-like 2. N Engl J Med 354:1370–1377. https://doi.org/10.1056/NEJMoa052773.

Swerdlow NR, Geyer MA (1993) Prepulse inhibition of acoustic startle in rats after lesions of the pedunculopontine tegmental nucleus. Behav Neurosci 107:104–117. https://doi.org/10.1037//0735-7044.107.1.104.

Swerdlow NR, Light GA, Thomas ML, Sprock J, Calkins ME, Green MF, Greenwood TA, Gur RE, Gur RC, Lazzeroni LC, Nuechterlein KH, Radant AD, Seidman LJ, Siever LJ, Silverman JM, Stone WS, Sugar CA, Tsuang DW, Tsuang MT, Turetsky BI, Braff DL (2018) Deficient prepulse inhibition in schizophrenia in a multi-site cohort: Internal replication and extension. Schizophr Res 198:6–15. https://doi.org/10.1016/j.schres.2017.05.013.

Wang HB, Tahara Y, Luk SHC, Kim Y-S, Hitchcock ON, MacDowell Kaswan ZA, In Kim Y, Block GD, Ghiani CA, Loh DH, Colwell CS (2020) Melatonin treatment of repetitive behavioral deficits in the Cntnap2 mouse model of autism spectrum disorder. Neurobiol Dis 145. https://doi.org/10.1016/j.nbd.2020.105064 105064.

Weber M, Schnitzler H-U, Schmid S (2002) Synaptic plasticity in the acoustic startle pathway: the neuronal basis for short-term habituation? Eur J Neurosci 16:1325–1332. https://doi.org/10.1046/j.1460-9568.2002.02194.x.

Xing X, Wu K, Dong Y, Zhou Y, Zhang J, Jiang F, Hu W-P, Li J-D (2020) Hyperactive Akt-mTOR pathway as a therapeutic target for pain hypersensitivity in Cntnap2-deficient mice. Neuropharmacology 165. https://doi.org/10.1016/j.neuropharm.2019.107816 107816.

Yeomans JS, Lee J, Yeomans MH, Steidl S, Li L (2006) Midbrain pathways for prepulse inhibition and startle activation in rat. Neuroscience 142:921–929. https://doi.org/10.1016/j.neuroscience.2006.06.025.

Zaman T, De Oliveira C, Smoka M, Narla C, Poulter MO, Schmid S (2017) BK Channels Mediate Synaptic Plasticity Underlying Habituation in Rats. J Neurosci 37:4540–4551. https://doi.org/10.1523/JNEUROSCI.3699-16.2017.

Zambricki EA, Dalecy LG (2004) Rat sex differences in anesthesia. Comp Med 54:49–53.

APPENDIX A. SUPPLEMENTARY MATERIAL

Supplementary material to this article can be found online at https://doi.org/10.1016/j.neuroscience.2023.01.020.

(Received 5 August 2022, Accepted 18 January 2023)
(Available online 25 January 2023)